High field transport in an edge overgrown lateral superlattice

Ç. Kurdak,[a] A. Zaslavsky,[b] D. C. Tsui, M. B. Santos,[c] and M. Shayegan
Department of Electrical Engineering, Princeton University, Princeton New Jersey 08544

(Received 22 September 1994; accepted for publication 16 November 1994)

We have realized by cleaved edge overgrowth a two-dimensional electron gas system in a one-dimensional lateral superlattice consisting of 100 periods of 120 Å GaAs/20 Å AlGaAs. These devices exhibit nonlinear $I-V$, including negative differential resistance, at high electric fields. We demonstrate, by monitoring the changes in the two-dimensional electron density, that the nonlinear $I-V$ is due to high field induced electron trapping. © *1995 American Institute of Physics.*

It was predicted by Bloch[1] that electrons in a periodic potential with an applied constant electric field would oscillate as a result of the Bragg reflections from zone boundaries. Esaki and Tsu[2] first proposed to use heterostructure superlattices (SL) to realize these high-frequency oscillations; they also predicted that the effect would lead to a negative differential resistance (NDR). Most of the earlier work is done on doped GaAs/AlGaAs SL where current carrying charges accumulate to form high field domains,[3] and only in undoped SL and in a special three-terminal SL structure high field negative differential velocity is observed.[4–6]

Recently, using a new crystal growth technique called cleaved edge overgrowth (CEO), Stormer *et al.*[7] demonstrated a new atomically precise lateral SL. CEO has significant advantages over other nanostructure fabrication techniques; it takes advantage of the atomic precision of molecular beam epitaxial (MBE) growth and does not suffer from surface depletion effects which can limit the precision of lithographic techniques. New lower dimensional electron systems and novel devices have already been realized using CEO.[7–13]

It is of fundamental interest to investigate Bragg reflection effects at high electric fields in these new lateral SL devices and compare the results to bulk SL devices. To this end, we designed a lateral SL structure with a Fermi level close to the top of the first miniband. The devices are realized by liquid phase epitaxial (LPE) CEO which we first demonstrated in the fabrication of a surface resonant tunneling diode.[8]

At low temperatures, unlike bulk SL devices, we have not observed high field domain formation in our SL devices suggesting that these lateral SL devices can deliver high currents without excess charge accumulation. Furthermore, unexpectedly, some of our SL devices exhibit a special kind of nonlinearity, including NDR, in the $I-V$ measurements where the $I-V$ characteristics of the devices change after application of high voltages. By carefully measuring the carrier density using magnetoresistance oscillations, we directly monitor the density of the two-dimensional (2D) electrons (n_{2D}) at the overgrown interface. We find that the change in the $I-V$ characteristics is associated with a reduction in the electron density and thus demonstrates that the observed nonlinearity is due to electron trapping.

Fabrication of these devices requires two crystal growth sequences. First, a superlattice structure is grown by MBE on a semi-insulating GaAs substrate with the following parameters: 8000 Å n^+-GaAs buffer layer (Si doped to 4×10^{17} cm^{-3}), 100 periods of undoped 120 Å GaAs/20 Å $Al_{0.2}Ga_{0.8}As$ superlattice, and a 4000 Å n^+-GaAs top contact layer (Si doped to 4×10^{17} cm^{-3}). Then, 5 mm×5 mm size samples from the MBE grown wafer are placed vertically on a specially designed graphite slider for LPE growth. Samples are cleaved by pushing the slider forward in the LPE chamber and Sn-doped AlGaAs is grown at 710 °C on the freshly cleaved interface. The regrown structure is cut into several samples with a typical width of 1 mm. The shallow top contact is made to the 4000 Å n^+-GaAs layer by evaporating and alloying a narrow strip of AuGeNiCr metal parallel to the cleaved edge; the bottom contact is made to the 8000 Å n^+-GaAs after wet etching through the SL by alloying In:Sn. A schematic cross-sectional diagram of the device is shown in Fig. 1(a). Note that the LPE-grown layer is typically thicker near the edge in LPE growth due to the different thermal conductivities of graphite and GaAs.[14,15]

The growth parameters of the device are chosen such that the Fermi level would be in close proximity to the top of the first miniband to enhance the miniband boundary effects in transport. Figure 1(b) shows the calculated dispersion in x direction using a standard 1D Kronig–Penney model using 120 Å wide wells, and 20 Å wide and 160 meV high barriers. The lowest miniband lies between 14.7 and 27.7 meV and is separated from the next miniband by 36 meV. Along the y axis the dispersion is quadratic. For our typical carrier density of $n_{2D}=4.1\times10^{11}$ cm^{-2}, the position of the Fermi level is close to the top of the miniband ($E_F=26$ meV), and the Fermi surface is anisotropic with $k_F^{(y)}=1.4\times10^6$ cm^{-1} and $k_F^{(x)}=1.8\times10^6$ cm^{-1}.

The results of two-point $I-V$ measurements from three samples at $T=4.2$ K are shown in Fig. 2(a). Samples 1A and 1B are from the same LPE growth whereas sample 2A is from a different growth. The measurements are done using a pulsed voltage ramp with a pulse width of 50 μs and a duty cycle of 0.05% to avoid sample heating. The solid lines show the initial $I-V$ obtained by sweeping the voltage up the first time after cooldown; all three of the devices exhibit nonlinear $I-V$, in particular sample 1B exhibits NDR around 1.3 V.

[a]Electronic mail: ckurdak@phoenix.princeton.edu
[b]Present address: Division of Engineering, Brown University, Providence, RI 02912.
[c]Present address: Department of Physics and Astronomy, University of Oklahoma, Norman, OK 73019.

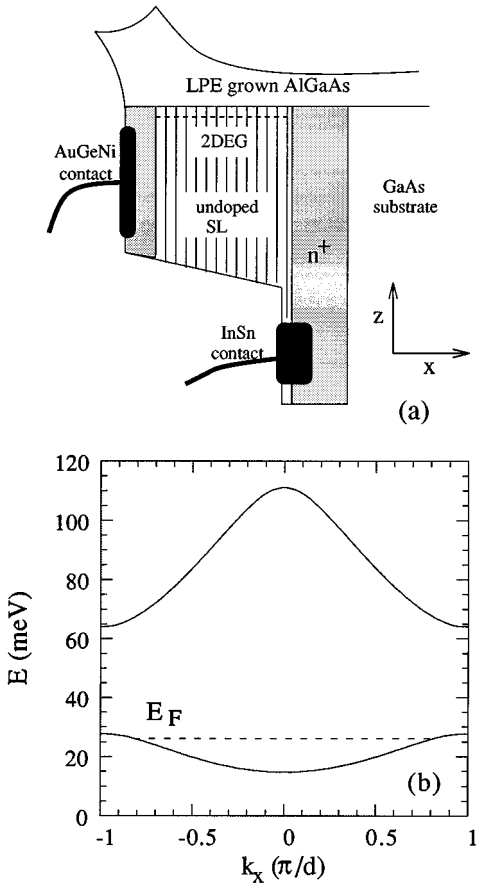

FIG. 1. (a) Schematic cross-sectional diagram of the edge-grown SL device (not to scale) and (b) calculated dispersion relation in x direction for this structure. Here, d is the period of the SL.

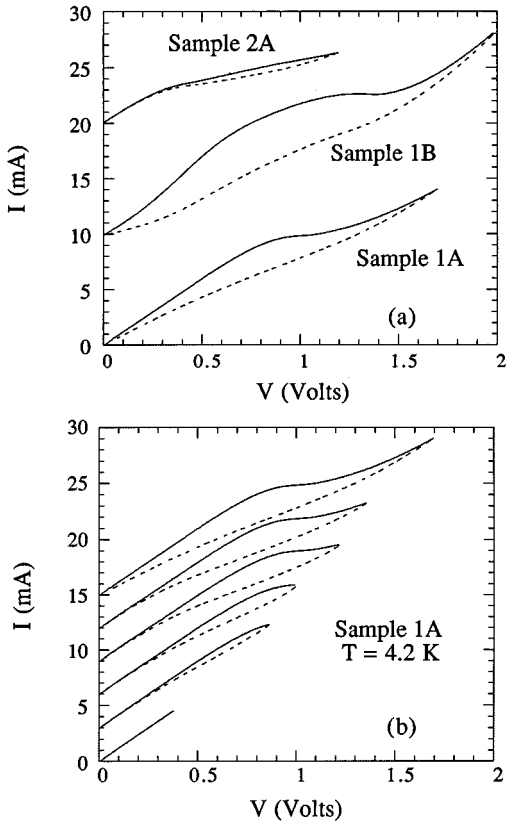

FIG. 2. $I-V$ characteristics of (a) three different samples; (b) sample 1A for different maximum applied voltages, at $T=4.2$ K. The curves from different samples in (a) and from different cooldowns in (b) are displaced upwards for clarity. Solid lines are from the first voltage sweep up after the cooldown and dotted lines are from the successive voltage sweeps.

More strikingly, $I-V$ characteristics change after this first voltage sweep, i.e., as the voltage is swept down and in the successive voltage sweeps, independent of the direction of the voltage sweep, the currents follow the lower dotted curves. After the change, the initial $I-V$ characteristics can be recovered by either shining red LED light or thermally cycling the sample to room temperature. We should note that these devices are very different from bulk SL devices in that they do not show high field domain formation which would lead to periodic NDR oscillations.[3] The superlinear $I-V$ observed in sample 1B at low voltages ($V<0.7$ V) is not seen in any of the other samples from this growth and is due to a contact problem. In the rest of this letter, we will focus on the data obtained from sample 1A and investigate the origin of the high electric field induced change in the $I-V$ characteristics.

The change in $I-V$ characteristics depends on the maximum applied voltage ($V_{\max}$). Figure 2(b) shows $I-V$ characteristics of sample 1A for different $V_{\max}$; each curve is obtained from a different cooldown of the sample. As shown in the bottom curve, the $I-V$ characteristic does not change if $V_{\max}$ is in the ohmic regime of the initial $I-V$. The upper curves show how the change in $I-V$ characteristics evolve as $V_{\max}$ goes beyond the ohmic regime.

In order to monitor the density of the 2D electrons at the overgrown interface, we performed two-point magnetoresistance measurements using standard lock-in detection at 17 Hz. Two typical magnetoresistance traces, one before (solid curve) and the other after the application of a high electric field, taken at $T=4.2$ K are shown in Fig. 3(a). The magnetic field (B) is perpendicular to the overgrown interface. The device exhibits Shubnikov-de Haas (SdH) oscillations which disappear if the sample is positioned with B lying in the plane of the overgrown interface as expected of the 2DEG. The change in the period of the SdH oscillations after the application of high electric field indicates that there is a reduction in n_{2D} which we attribute to the electric field induced trapping of electrons. From the period of the SdH oscillations we obtain an initial $n_{2D}=4.1\times10^{11}$ cm^{-2}, which remains the same for different cooldowns. However, the final n_{2D} as shown in Fig. 3(b) depends on the maximum applied voltage. Note that every point in Fig. 3(b) is obtained from a different cooldown of the sample. If the maximum applied voltage is in the linear regime of the device ($V_{\max}<0.8$ V), no change in n_{2D} is observed. On the other hand, for $V_{\max}>0.8$ V, we observe a decrease in n_{2D}. Since the sample resistance (R) is a function of n_{2D}, in this voltage range R is a function of applied voltage. A nonlinear $I-V$ is expected to result from such a decrease in n_{2D}. This is consistent with the observed nonlinearity in the $I-V$ characteristics of the device. For applied voltages higher than 2 V, the 2D electron density

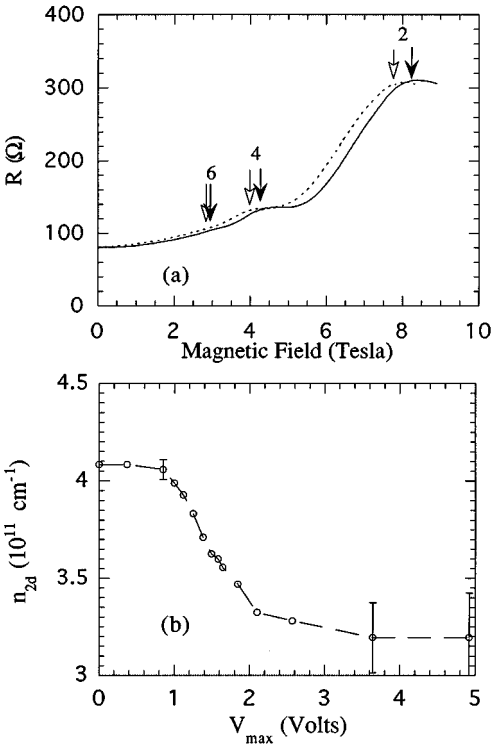

FIG. 3. (a) Two-point resistance of sample 1A as a function of magnetic field (applied along z direction) at $T=4.2$ K. The solid trace was taken just after the cooldown and the dotted line was taken after the application of a high voltage ($V_{\max}=1.1$ V). Because of the aspect ratio of the 2DEG, our sample geometry is equivalent to the Carbino geometry which measures $1/\sigma_{xx}$. The arrows indicate Landau level filling factors 2, 4, and 6. (b) The final carrier density after application of high electric fields as a function of the maximum applied voltage. Each point is obtained from a different cooldown of the sample.

does not decrease any lower than 3.2×10^{11} cm^{-2} and, in this voltage range, the $I-V$ characteristics of the device does not change after the first voltage sweep (not shown).

From these observations, we conclude that, triggered by high electric fields, some of the electrons are trapped and this electron trapping is the origin of the high field nonlinearity observed in this device. The exact nature of these traps has not been identified yet.

We repeated the same measurements on sample 1B from the same LPE growth and showed that the NDR observed in this device is also due to similar trapping effect. This sample has the same n_{2D} of 4.1×10^{11} cm^{-2} before the application of high fields and n_{2D} decreases in a similar fashion with $V_{\max}$. For example, for the data shown in Fig. 2(a) the carrier density of sample 1B decreased to 3.5×10^{11} cm^{-2} after the voltage sweep. On the other hand, sample 2A is from a different growth and shows a well pronounced nonlinearity at $V=0.3$ V. This nonlinearity is different in that it persists (actually becomes more pronounced) after the application of high voltages and, furthermore, no significant change in ohmic resistance is observed. Unfortunately, we could not monitor the 2D electron density for this sample, since the magnetoresistance of this sample does not exhibit SdH oscillations. This might be either due to low electron mobility or due to an open Fermi surface which can happen in a lateral SL if the electron density is high enough to totally fill the first miniband.

In conclusion, we systematically studied $I-V$ characteristics of lateral SL devices fabricated by the LPE overgrowth technique. These devices behave differently from bulk SL devices in that they do not form high field domains. We also observed an unexpected decrease in current at high electric fields which we showed to be caused by trapping of 2D electrons.

The authors would like to thank K. Hirakawa for many helpful discussions and C.-H. Kuan for the Kronig–Penney calculation. This work was supported by the ONR and the NSF.

[1] F. Bloch, Z. Phys. **52**, 555 (1928); Bloch oscillator is recently realized: C. Waschke, H. G. Roskos, K. Leo, H. Kurz, and K. Kohler, Semicond. Sci. Technol. **9**, 416 (1994).
[2] L. Esaki and R. Tsu, IBM J. Res. Dev. **14**, 61 (1970).
[3] K. K. Choi, B. F. Levine, R. J. Malik, J. Walker, and C. G. Bethea, Phys. Rev. B **35**, 4172 (1987); L. Esaki and L. L. Chang, Phys. Rev. Lett. **33**, 495 (1974).
[4] A. Sibille, J. F. Palmier, C. Minot, and F. Mollot, Appl. Phys. Lett. **54**, 165 (1989); A. Sibille, J. F. Palmier, H. Wang, and F. Mollot, Phys. Rev. Lett. **64**, 52 (1990).
[5] H. T. Grahn, K. von Klitzing, K. Ploog, and G. H. Dohler, Phys. Rev. B **43**, 12 094 (1991).
[6] F. Beltram, F. Capasso, D. L. Silvo, A. L. Hutchinson, S.-N. G. Chu, and A. Y. Cho, Phys. Rev. Lett. **64**, 3167 (1990).
[7] H. L. Stormer , L. N. Pfeiffer , K. W. Baldwin , K. W. West , and J. Spector , Appl. Phys. Lett. **58**, 726 (1991).
[8] A. Zaslavsky, D. C. Tsui, M. Santos, and M. Shayegan, Appl. Phys. Lett. **58**, 1440 (1991).
[9] L. N. Pfeiffer, K. W. West, H. L. Stormer, J. P. Eisenstein, K. W. Baldwin, D. Gershoni, and J. Spector, Appl. Phys. Lett. **56**, 1697 (1990).
[10] H. L. Stormer, K. W. Baldwin, L. N. Pfeiffer, and K. W. West, Appl. Phys. Lett. **59**, 1111 (1991).
[11] J. Motohisa and H. Sakai, Appl. Phys. Lett. **63,** 1786 (1993).
[12] Ç. Kurdak, D. C. Tsui, S. Parihar, M. B. Santos, H. C. Manoharan, S. A. Lyon, and M. Shayegan, Appl. Phys. Lett. **64**, 610 (1994).
[13] W. Wegscheider, L. N. Pfeiffer, M. M. Dignam, A. Pinczuk, K. W. West , S. L. McCall, and R. Hull, Phys. Rev. Lett. **71**, 4071 (1993).
[14] D. L. Rode and R. G. Sobers, J. Cryst. Growth **29**, 61 (1975).
[15] M. R. Frei, Ph.D. thesis, Princeton University, 1990.